

Original Article

Design and Performance Analysis of Polarization Reconfigurable Antenna using a Hybrid Coupler

Bammidi Deepa^{1*}, K Chandra Bhushana Rao²

¹Department of ECE, JNTU Kakinada, Kakinada, Andhra Pradesh, India.

²Department of Electronics and Communication Engineering, JNTUGV, Andhra Pradesh, India.

¹Corresponding Author : deepabammidi2024@gmail.com

Received: 03 June 2025

Revised: 05 July 2025

Accepted: 04 August 2025

Published: 30 August 2025

Abstract - Antennas for wireless signals must be reconfigurable because these detectors need to deal with several polarization options to enhance the link's reliability and limit loss. The antenna system proposed in this study works at S-band frequencies between 2.1 and 2.8 GHz. The configuration is novel since a hybrid coupler allows linking two networks via a dual-layer antenna consisting of a network and a patch element printed over FR4. This hybrid coupler allows precise control over the current distribution in the patch and, as a result, allows this device to transition between polarization states continuously, including LP, LHCP and RHCP. Conversion from circular to linear polarization is achieved by manipulating the phase using a matrix of well-positioned PIN diode switches (SMP1345-079LF). This single-feed configuration allows some flexibility in operations and guarantees that performance in polarization is given to equal reliability, independent of the mode being excited. From the performance analysis, the antenna achieves approximately 6dB of gain and remains operational at a consistent level within the desired frequency band. Due to its versatility, the design can be useful in the S-band spectrum, wireless networks, navigation, meteorology, and aviation surveillance for air traffic management, improving the performance of the systems and requiring less hardware than earlier solutions.

Keywords - PIN diodes, Polarization reconfigurable antenna, Hybrid coupler, Theory of characteristic modes, Two-layered antennas.

1. Introduction

Reliable antenna engineering has depended on electromagnetic simulation tools for over ten years present times Finite element solvers represent one of the most popular numerical methods of analyzing and simulating complex electromagnetic structures in terms of Maxwell equations solved on the discretized domains; it applies to Finite Element Method (FEM), Finite-Difference Time-Domain (FDTD), and Method of Moments (MoM) case. With the aid of the latest finite element solvers, large structures can be handled, the material to be used can be chosen, and different targeted frequencies, overall computational costs and mesh details can also be estimated from these new tools. The authors discussed antennas that generate circular polarization by separating each signal by 90 degrees, keeping high port separation, and allowing RF signals to be flipped for a different polarization [1]. An attempt has been made to incorporate performing parts in ground planes and use PIN diodes to switch between linear, RHCP and LHCP polarization states [2]. As pointed out by Vinayagam et al., such adaptive systems help modern wireless networks remain flexible and adaptable [3]. Yuan et al. suggest that by choosing a rectangular patch shape, the polarization can be switched using the TM10 and TM20

transverse magnetic modes [4]. Xiao et al [5] described a system combining waveguides with circular polarization properties, using elements that stop signals within the 24- 48 GHz range. The work described by the authors of [6] employed the 5.8-6.3 GHz band to develop a design that changes polarity, leading to a 10% change in impedance and showing omnidirectional performance when the antenna is operating at 67° and 120° in the E-plane. The researchers in [7] made it possible by switching between polarizations and steering the beam using multilayer ceramic capacitors and integrated circuit inductors. Researchers at [8] have developed a dual-feed microstrip antenna that delivers circular or linear polarization over 2.25 to 2.6 GHz. Valdes et al [9] employed Germanium Telluride to design reconfigurable antennas that function with millimetre-wave technologies. Liu then presented [10] a remarkable antenna design in a mushroom shape that can vary between circular and linear polarization modes. A miniature, Christmas tree-shaped microstrip textile antenna from Salma et al is designed and analyzed with a detailed focus on flexibility, compactness, and adaptation of wearable communication systems [11]. Zhang et al. [12] explored how to use non-uniform partially reflective surfaces for a wide collection of multi-linear polarization states. The



authors of [13] examined using liquid gallium-indium alloys to design antenna patterns. Sandeep et al conducted a comprehensive study encompassing material selection, design, and modeling of a conformal circularly polarized textile antenna, specifically optimized for wearable applications with enhanced flexibility, durability, and polarization stability [14]. Huang et al [15] introduced broadband array structures that operate in both the C and S frequency bands and give full polarization switching ability. Yang et al. [16] presented meta-materials and examples of controlling them in antenna systems. Htun et al. used the proximity gap-coupled branches together with the simple bias-decoupling mechanism to achieve polarization reconfigurability [17]. Sangeetha et al. discussed the different applications of reconfigurable antennas and their performance metrics [18]. The authors looked at a circularly polarized hybrid reconfigurable textile antenna and demonstrated its performance and versatility in body-centric environments for applications in wearable biomedical and communications use [19]. Yang et al. have brought a reduction in switches on RA through the adoption of the IMPM method [20].

Novelty of the work is that an innovative means of integration of the hybrid coupler makes it possible to provide the possibility of polarization flexibility in the design of an antenna, which is less studied in the literature, and the majority of works are based on the use of conventional switching elements or rotation. The proposed antenna is unlike standard designs, where switching between linear and circular polarization is achieved with a complex circuit; the proposed antenna improves flexibility in polarisation-mismatched environments. Besides, a hybrid coupler design is expected to provide superior isolation, phase balance, and compactness that demonstrates superior performance with metrics like return loss, axial ratio, gain and polarization over the multi-band frequencies. The design not only reduces the complexity of the reconfiguration mechanism but also attains better performance efficiency than previous implementations.

2. Antenna Design Structure

Taking advantage of HFSS simulation after the antenna design, it was improved by systematically tuning parameters to achieve better isolation and purity of polarization, which led to an increase in gain. Many simulations were run using HFSS to obtain a thorough range of data from the parametric sweep analysis. Parametric optimization was based on three important geometric values: the length of the radiator on the first feeder patch (Lp), the radiator length on the secondary patch, which is parasitic in nature (Lp2) and the spacing of radiators (d) on the secondary surface. These parameters were chosen because they strongly affect the antenna's electromagnetic performance for microwave communication systems. Results from both sets of simulations were compared by mostly paying attention to isolation and polarization purity factors. Increasing the antenna's performance by using the systematic parameter tuning method proved to be effective in

boosting the performance of microwave antennas. Figures 1(a), and 1(b) illustrate the suggested antenna structure for the polarisation-reconfiguration antenna, including a parasitic patch. Radiation patch and feeding network are the top layer of an antenna structure. The antenna is made of two layers using an FR4 substrate. The thickness of each substrate is 1.6mm, and both are made from FR4 material. Two layers of the antenna have two patch layouts. Figure 1(d) shows the two-element parasitic patch with two square patches as the radiators. Figure 1(c) demonstrates a hybrid coupler-connected feed system, managed by PIN diodes. Modern systems for communication have made it important to study the performance characteristics of two-layer microstrip antennas. Integrating a hybrid coupler on the chip's lower surface strengthens these feeding capacities. The system must be designed this way to support dual polarization, a wide bandwidth and a good shape for its radiation.

Figure 1(e) shows that two diodes are mounted on the hybrid coupler on the driven patch; simulators use the names S1 and S2 for them. Shifting the diodes on the two patch structures rearranges the power distribution and enables the antenna to radiate in different directions. The two layers are designed using FR4 substrates and have physical features of 200 mm by 150 mm, 1.6 mm in thickness and a dielectric constant (ϵ_r) of 4.4. Figure 2 illustrates the presence of the feed line, linked to the hybrid coupler found on substrate-1.

The image in Figure 3 represents the structure of the designed two-layer antenna. By looking at Figure 4 from the side view, it can be understood that the two SMP 1345-079LF diodes were used to build the driven patch. Precautionary steps are applied to decrease the radiation resulting from soldering the diodes and related wires. Each dimension of the antenna has been chosen specifically for applications at the S-band frequency. The electromagnetic reference and support are adequate because of the size of the ground plane ($W_g = 150$ mm, $L_g = 200$ mm).

As top performance is important, the arrangement of feeders and radiators changes between the lower and upper patch designs. The double-layered structure is designed so that each radiating element on the feeder patch has 80 mm (d) of space between them for proper electromagnetic coupling. The precise measurement of sizes in the hybrid coupler network is important for obtaining the needed impedance between various phases. Improving impedance transformation across various regions is made possible by coupling with two sizes: 3.2 mm (W50) and 5.2 mm (W35). The coupler is designed with a main dimension L1 of 19 mm, giving the needed quarter-wavelength at the frequency it uses. As a result, antennas can achieve optimum electromagnetic results, perfect impedance, and smoothly distributed power while still being small. The fabricated antenna front view and the rear view can be seen in Figures 5(a) and 5(b). The VNA was used to find its S11 and VSWR values, as shown in Figure 6(a), to

know the near field response of the designed antenna. Far field measurements, including the antenna's gain and radiation

pattern, were captured in an anechoic chamber, as shown in Figure 6(b).

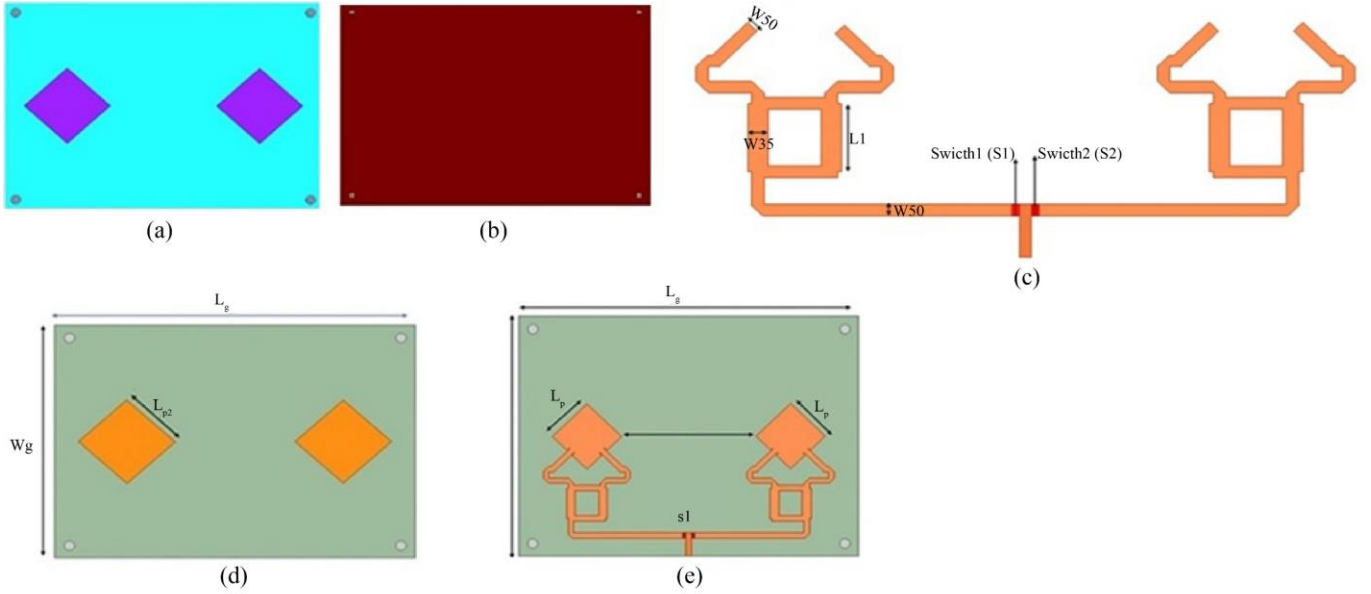


Fig. 1(a) Two-element parasitic patch on Substrate-2, (b) Ground Structure of the antenna below substrate-1, (c) Hybrid coupler design to feed input to the active patch, (d) Two-element structure on the patch on the parasitic substrate, and (e) Two-element structure in simulation on the driven patch connected to the hybrid coupler with PIN diodes working as switches S1 & S2, Example for a small figure.

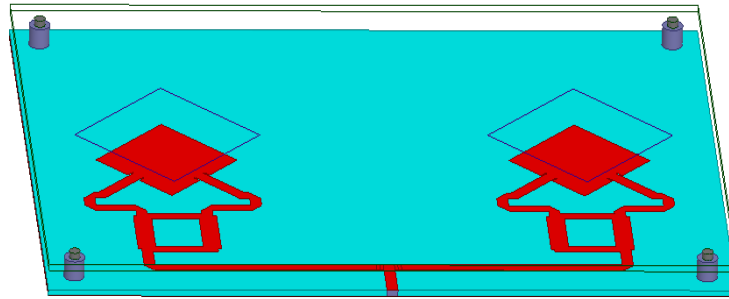


Fig. 2 Two-element patch on active substrate-1

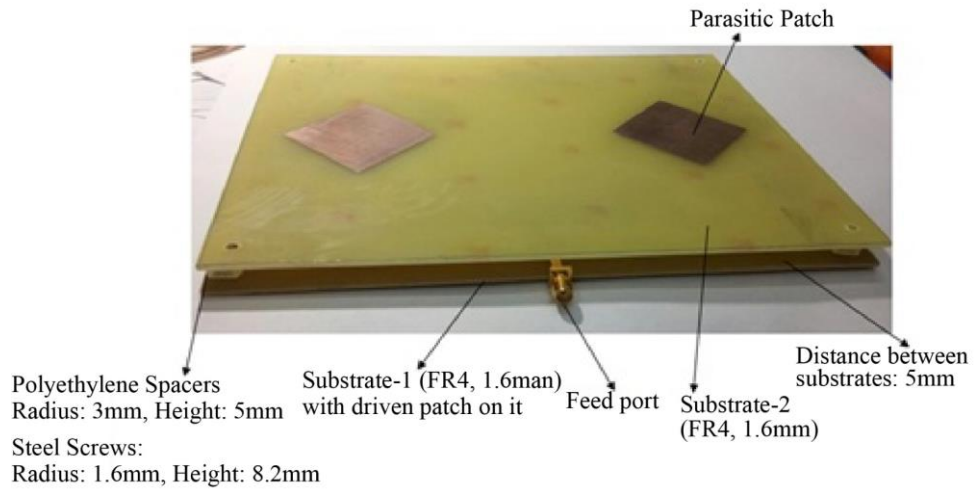


Fig. 3 Fabricated antenna with two substrates and one feed

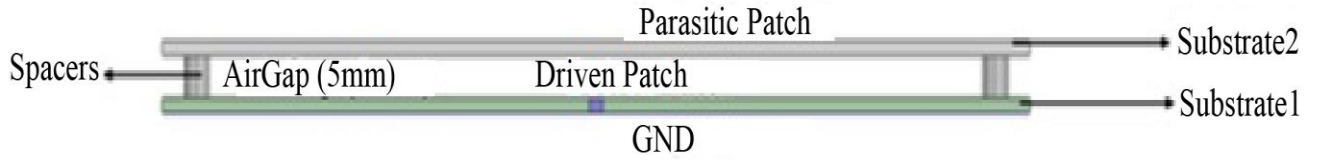


Fig. 4 Side view of the antenna

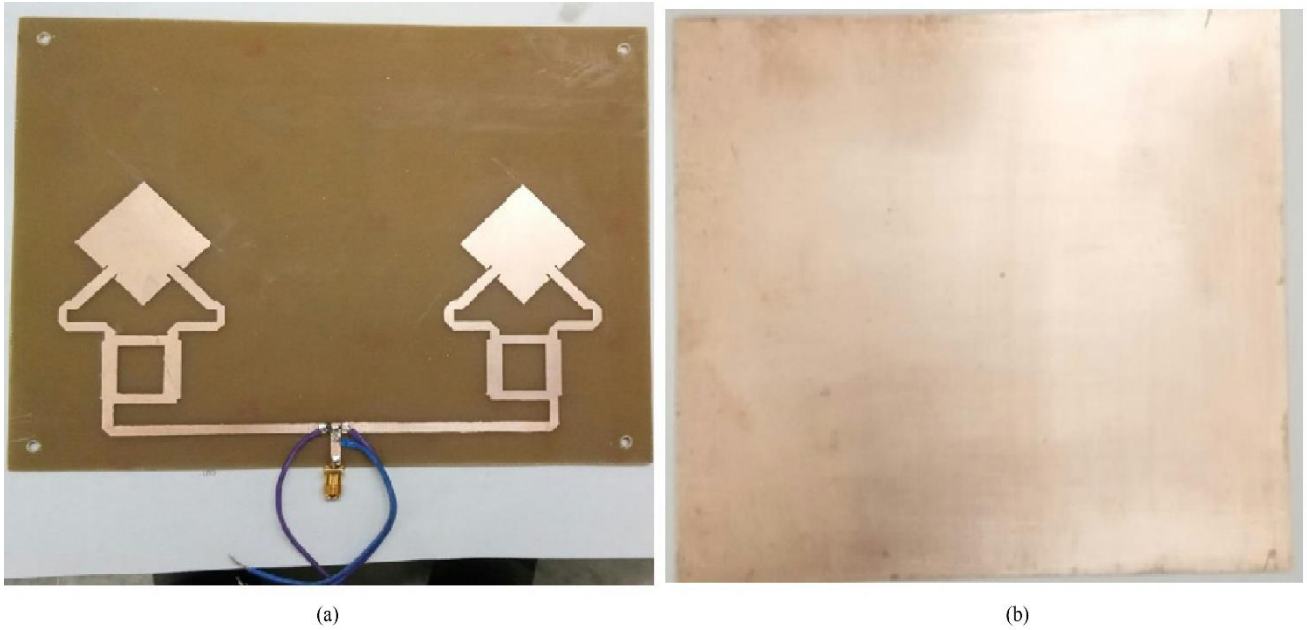


Fig. 5(a) Fabricated driven patch with two PIN diodes soldered on it, and (b) Ground structure of the fabricated antenna.

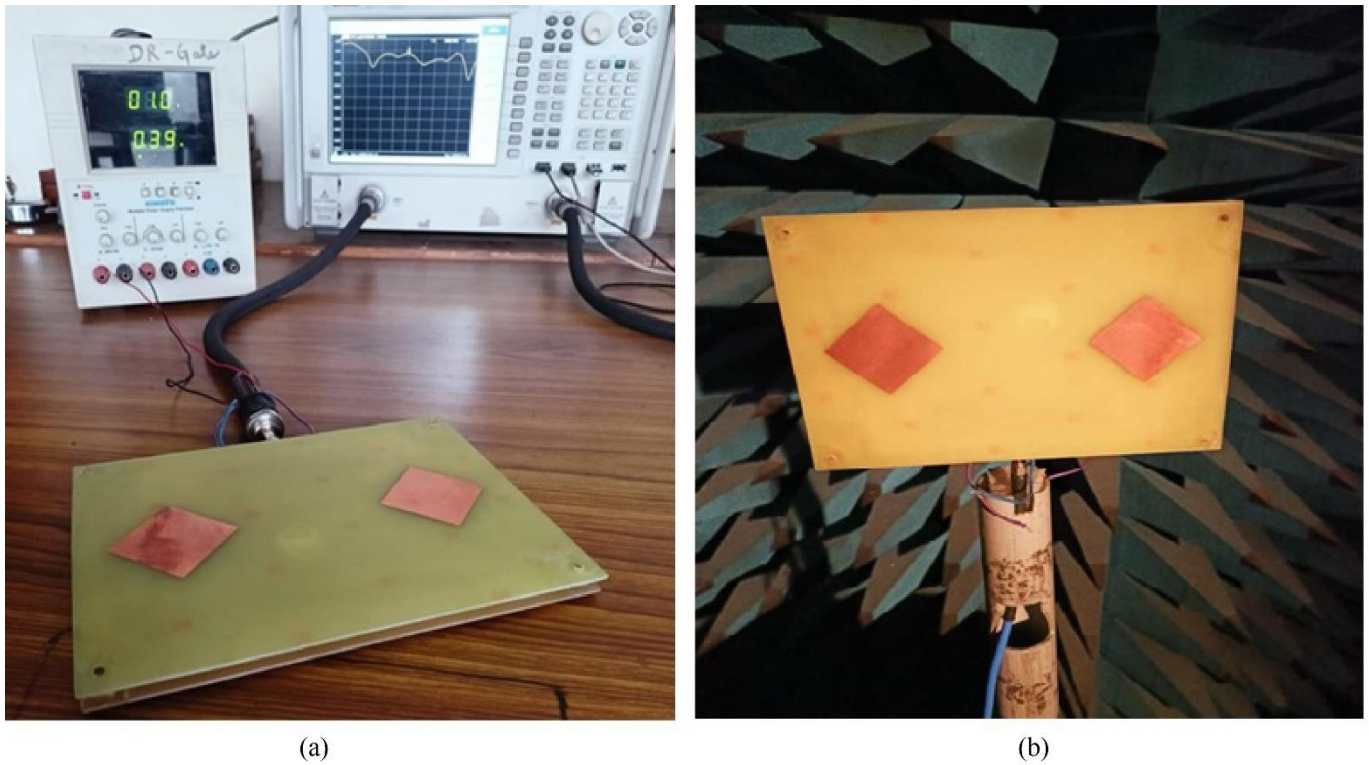


Fig. 6(a) VNA Test on the fabricated antenna, and (b) Tests in an anechoic chamber using the manufactured antenna.

3. Results and Discussions

The result plots of the antenna are shown in Figures 7(a) and 7(b), with its reflection coefficient less than -10dB for simulation and fabrication, respectively. If a match between components, such as a transmitter and an antenna or between a cable and a connector, is good, the symbol will have a value of -10 dB. System operation is made efficient, and the best power is sent through proper matching, as can be observed for the switching case-1, the simulation and the fabrication results of the antenna almost match. Acceptable bandwidth for a 0.7GHz antenna in polarization reconfigurable antenna is provided if polarization purity remains high and the antenna

continues to have high gain. In case 2, switching happens between 2.2 GHz and 2.87 GHz, making the bandwidth 0.67 GHz and the centre frequency 2.54 GHz. Figures 8(a) and 8(b) show the simulation and fabricated antenna results, respectively. With D1 and D2 operating, the simulated antenna's S11 plot (Figures 9(a) and 9(b)) reveals its functioning bandwidth is from 2.15 GHz to 2.79 GHz, with 0.64 GHz of bandwidth. Besides, the S11 value is at most -31.89 dB, and there is a noticeable notch between 2.34 GHz and 2.58 GHz. Figures 9(a) and 9(b) present the simulation and fabricated antenna result plots, respectively, which show a very good match between their response.

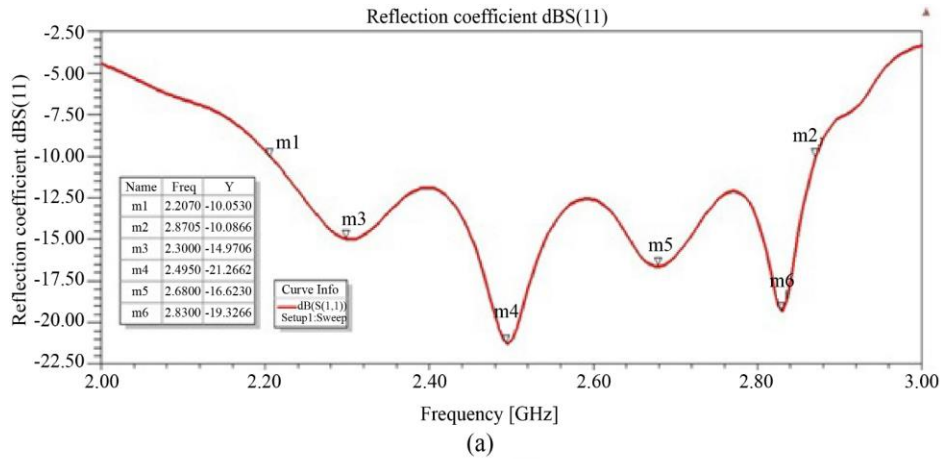


Fig. 7(a) S11 plot of simulated antenna when D1 OFF & D2 ON, and (b) S11 plot of the simulated antenna, plotted on VNA when D1 is OFF and D2 is ON.

When one of these components (D1) is not enabled and the other (D2) is enabled, its electric field distribution is studied, as shown in Figure 10(a). When D1 is off and D2 is on, two switch settings are available in the antenna system. The presence of many variables, for example, the size and shape of your antenna, its material composition and the input signal's strength and frequency, will control the way the electric field is shaped and how strong it is. An arm of the hybrid coupler allows us to observe the electric field

distribution on one side of the cat, which leads to LHCP. You can see from Figure 10(b) that an electric field drives the loop antenna on its left side, which flows through one of the hybrid coupler's sections, producing the RHCP radiation. The arrangement of the electric field around both feed lines and hybrid coupler arms, shown in Figure 10(c), suggests that the antenna can produce linear polarization. When D1 is off and D2 is on, the gain is boosted by 6.4 dB, seen in Figure 11(a). Most of the antenna's energy is directed out of the main lobe.

Better signal strength and longer distance are possible thanks to increased power in the main direction from high-gain antennas. In the conditions of Figure 11(b), antenna gain

amounts to 6.67dB with D1 on and D2 off. When both diodes are activated, the radiated power of the antenna is reported as having a gain of 5.44dB see Figure 11(c).

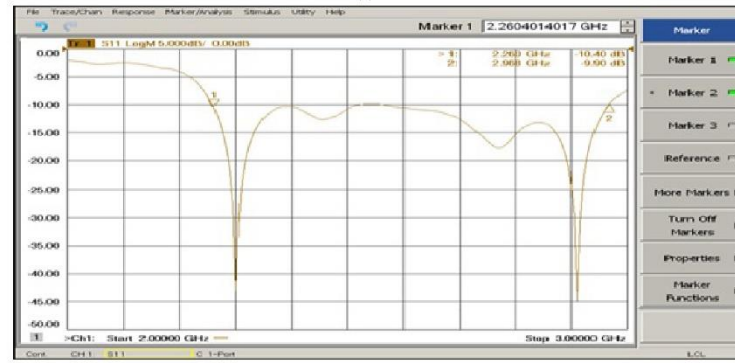
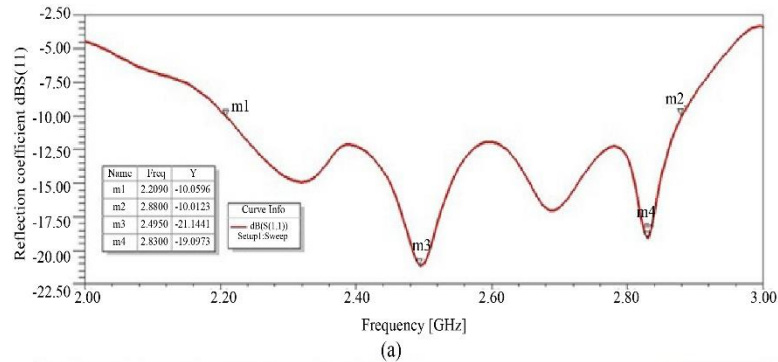


Fig. 8(a) S11 plot of simulated antenna with D1 ON & D2 OFF, and (b) S11 plot of the fabricated antenna with D1 ON & D2 OFF.

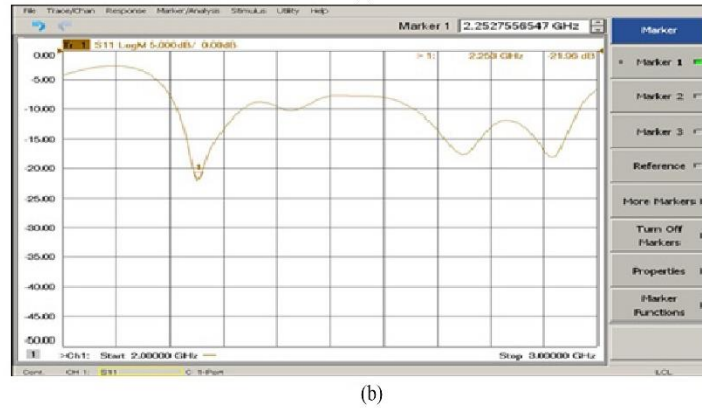
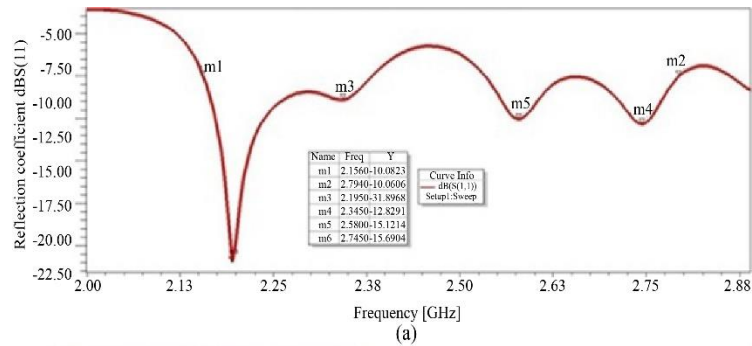


Fig. 9(a) S11 plot of the simulated antenna with D1, D2 ON, and (b) S11 plot of the fabricated antenna with D1, D2 ON.

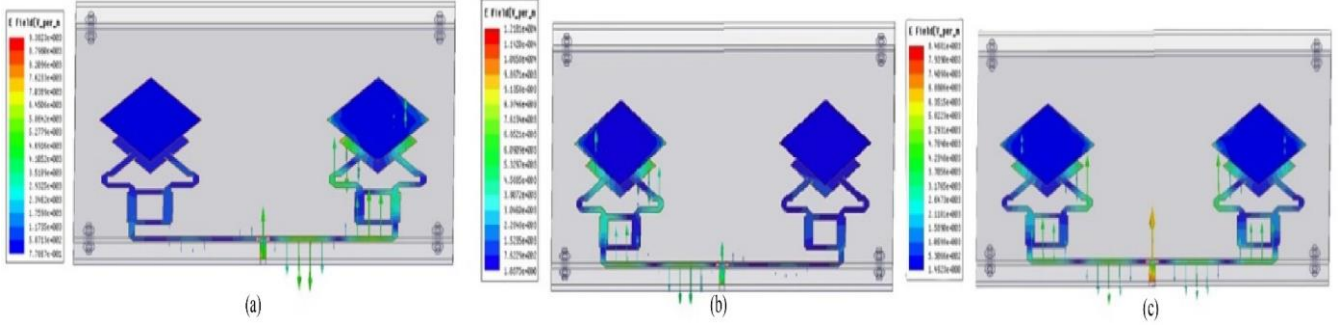


Fig. 10(a) Electric field distribution of simulated antenna with D1 OFF & D2 ON, (b) Current density distribution of the simulated antenna with D1 ON & D2 OFF, and (c) Electric field distribution of antenna when D1, D2 are ON, displaying linear polarization.

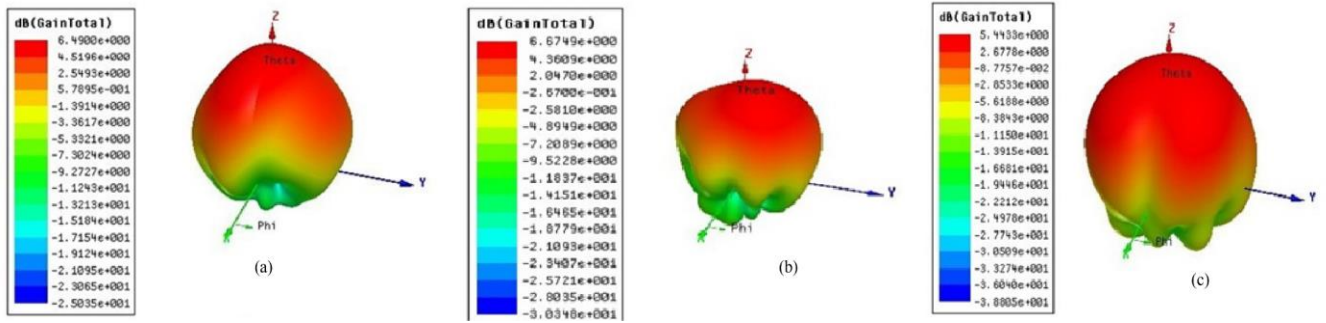


Fig. 11(a) Gain plot of the antenna with D1 is OFF and D2 is ON, (b) Gain of the simulated antenna with D1 ON & D2 OFF, and (c) Gain of the simulated antenna with D1, D2 ON, displaying linear polarization.

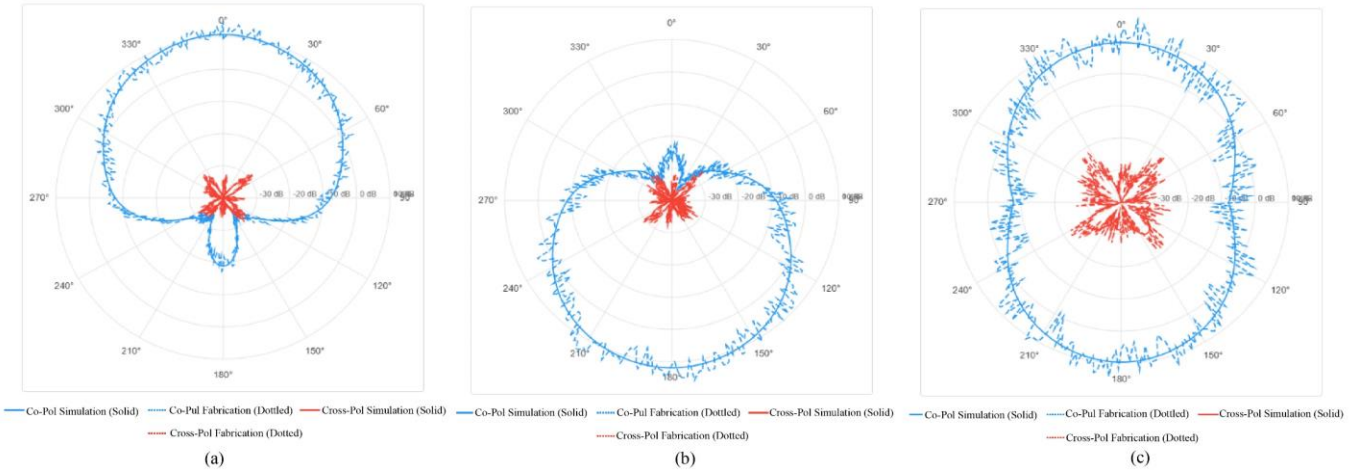


Fig. 12(a) E-field plot of the antenna with D1 is OFF and D2 is ON (LHCP), (b) E-field plot of the antenna with D1 is ON and D2 is OFF (RHCP), and (c) E-field plot of the antenna with D1 is ON and D2 is ON (LP).

In case -1, with D1 turned off and D2 turned on, the LHCP radiation direction of the far-field radiation polarization reconfigurable antenna is shown in Figure 12(a). During case -2, with D1 on and D2 off, the far-field radiation polarization reconfigurable antenna displays RHCP radiation as in Figure 12(b). With both PIN diodes turned ON in the third switching state, linear polarization of the antenna is observed, as can be seen in Figure 12(c). As a result, the measured results in Figure 12 confirm that the antenna can be easily switched between polarization states, with excellent gain performance and obvious differences between co- and cross polarization.

We also observe that the fabricated antenna results match the simulations. The state of polarization in the traditional antenna systems can be linear, circular, or elliptical, but it will remain constant during the design time. These antennas do not have sufficient flexibility to work in different propagation conditions, particularly in an operating environment in which there is a polarization mismatch problem between the transmitter and the receiver, creating extreme signal degradation. This rigid polarization transmission limits the performance of the antenna in unpredictable, dynamic, and multipath-rich applications systems. As shown in Table 1, the

proposed work implements polarization reconfigurability and the antenna acquires the ability to switch between various polarization modes dynamically. Achieves broad bandwidth (708 MHz) with compact dual-layer FR4 design, enhanced

polarization diversity (LHCP, RHCP, LP), and superior S11 (-45 dB), outperforming other works in bandwidth, polarization flexibility, and impedance matching.

Table 1. Comparison of the findings with state-of-the-art approaches

Measurement Metric	Presented Work	Ref. [3]	Ref. [4]	Ref. [6]	Ref. [7]	Ref. [8]
Material	FR4	FR4	Rogers R04003C	Rogers R04003C	RO4350B	FR4
Dimensions	150x200mm	60x60mm	110 mm × 110 mm × 10 mm.	60x50mm	31x31mm	42x13.8mm
Reconfigurability	Polarization	Polarization	Polarization	Polarization	Polarization	Polarization
S11	-45dB (least)	-24dB	-22dB	-22dB	-35dB	-32dB
Polarization	LHCP, RHCP,LP	LHCP, RHCP	Linear TM10, TM20	LHCP and RHCP	LHCP and RHCP	LHCP, RHCP,LP
Gain	6.49dB	5dB		5.78dB	7dB	6.8 dB
Frequency	2.1-2.8GHz (BW: 708MHz)	4.7 GHz BW:100Mz	2.15 - 2.94GHz	5.8-6.3 GHz (0.5GHz)	5.25-5.6GHz (0.35Ghz)	2.25-2.60GHz (0.35GHz)
Number of layers	2	1	2	2	2	2

4. Conclusion

An antenna that can switch polarisation has been developed by creating a simple feeding network for reconfigurability with only two PIN diodes and a hybrid coupler. The opening of the antenna uses four square rings set up in two horizontally and vertically, so the antenna is small but works as well. It has been made so that it operates in Linear Polarized (LP) or Left-Hand Circular Polarized (LHCP) or Right-Hand Circular Polarized (RHCP) conditions. The frequency band from 2.44 to 2.47 GHz has been checked experimentally, and the measured broadside gain is approximately 6.5 dB. Due to the limited access to diodes, adding new polarization states to existing antennas makes the bias network more complicated and increases radiation, but the new antenna offers multiple polarization states using far fewer diodes and keeps the bias network simpler. Unlike several existing studies that employ complex Substrate Integrated Waveguide (SIW) architectures and microcontroller-based switching networks for achieving polarization reconfigurability, the proposed design introduces a novel hybrid coupler-based signal distribution mechanism. The use of a hybrid coupler significantly simplifies the feeding structure while ensuring efficient power distribution across the radiating elements. This approach enhances integration ease,

reduces circuit complexity, and improves overall radiation performance. Furthermore, the antenna demonstrates enhanced versatility by supporting multiple polarization states (LHCP, RHCP, and LP) with improved impedance matching and broader bandwidth, thereby establishing its superiority in terms of practical applicability and performance. The authors have also discussed other antenna structures in previous publications, but the work discussed in this paper is not at all related to that work. A major issue that is observed while designing the reconfigurable antennas lies in the usage of the switching of PIN diodes, which are quite significant. The main challenges are how to bias network design, not influence the RF performance, minimize parasitic effects, keep the ark at a stable temperature, and prevent signal distortion when switching. Also, PIN diodes can have unwanted nonlinear characteristics at even higher frequencies, producing undesired harmonics and impedance mismatch. However, these issues can be reduced by proper layout design, having RF chokes with high isolation, planning the layout to decouple the DC and RF signal, and designing with an optimum biasing circuit. Surface-mount technology and appropriate thermal control further guarantee dependable and reliable performance, supplying the ability to regulate the reconfigurable states of the antenna closely.

References

- [1] Constantine A. Balanis, *Antenna Theory: Analysis and Design*, 3rd ed., A John Wiley & Sons, Hoboken, New Jersey, 2005. [[Google Scholar](#)] [[Publisher Link](#)]
- [2] Ramesh Garg et al., *Microstrip Antenna Design Handbook*, Artech house, Boston, London, 2001. [[Google Scholar](#)]
- [3] Kanniyappan Vinayagam, and Rajesh Natarajan, "Polarization Reconfigurable Patch Antenna Using Parasitic Elements for Sub-6 GHz Applications," *International Journal of Electrical and Computer Engineering Systems*, vol. 16, no. 1, pp. 1-7, 2024. [[CrossRef](#)] [[Google Scholar](#)] [[Publisher Link](#)]

- [4] Xianjing Yuan et al., "A Wideband Polarization-Reconfigurable Antenna Based on Fusion of TM₁₀ and Transformed-TM₂₀ Mode," *Electronics*, vol. 13, no. 18, pp. 1-12, 2024. [[CrossRef](#)] [[Google Scholar](#)] [[Publisher Link](#)]
- [5] Jun Xiao et al., "High-Gain and Low-Cost Circularly Polarized Antenna Array for 5G MMW Applications," *IET Microwaves, Antennas & Propagation*, vol. 16, no. 2-3, pp. 174-184, 2022. [[CrossRef](#)] [[Google Scholar](#)] [[Publisher Link](#)]
- [6] Haoran Zhao, Binyun Yan, and Weixing Sheng, "A Beamwidth and Beam Direction Reconfigurable Antenna based on Multi-Mode Parasitic Coupling," *IET Microwaves, Antennas & Propagation*, vol. 18, no. 8, pp. 578-584, 2024. [[CrossRef](#)] [[Google Scholar](#)] [[Publisher Link](#)]
- [7] Chao Liu et al., "Polarization Reconfigurable and Beam-Switchable Array Antenna Using Switchable Feed Network," *IEEE Access*, vol. 10, pp. 29032-29039, 2022. [[CrossRef](#)] [[Google Scholar](#)] [[Publisher Link](#)]
- [8] Shenyn Wang et al., "Polarization-Reconfigurable Antenna Using Combination of Circular Polarized Modes," *IEEE Access*, vol. 9, pp. 45622-45631, 2021. [[CrossRef](#)] [[Google Scholar](#)] [[Publisher Link](#)]
- [9] Jehison Leon Valdes et al., "A Polarization Reconfigurable Patch Antenna in the Millimeter-Waves Domain Using Optical Control of Phase Change Materials," *IEEE Open Journal of Antennas and Propagation*, vol. 1, pp. 224-232, 2020. [[CrossRef](#)] [[Google Scholar](#)] [[Publisher Link](#)]
- [10] Peng Liu et al., "Broadband and Low-Profile Penta-Polarization Reconfigurable Metamaterial Antenna," *IEEE Access*, vol. 8, pp. 21823-21831, 2020. [[CrossRef](#)] [[Google Scholar](#)] [[Publisher Link](#)]
- [11] Salma Syed et al., "Christmas-Tree Shaped Compact Microstrip Textile Antenna for Telemetry, ISM and X-band Applications," *Materials Today: Proceedings*, vol. 80, pp. 1665-1670, 2023. [[CrossRef](#)] [[Google Scholar](#)] [[Publisher Link](#)]
- [12] Yuwei Zhang et al., "Wideband Pattern and Polarization-Reconfigurable Antenna Based on Bistable Composite Cylindrical Shells," *IEEE Access*, vol. 8, pp. 66777-66787, 2020. [[CrossRef](#)] [[Google Scholar](#)] [[Publisher Link](#)]
- [13] Yi Zhou et al., "A Liquid-Metal-Based Crossed-Slot Antenna with Polarization and Continuous-Frequency Reconfiguration," *IEEE Open Journal of Antennas and Propagation*, vol. 3, pp. 1102-1108, 2022. [[CrossRef](#)] [[Google Scholar](#)] [[Publisher Link](#)]
- [14] D. Ram Sandeep et al., "Material Selection to Modeling: A Comprehensive Investigation of a Conformal Circularly Polarized Textile Antenna for Wearable Applications," *IEEE Access*, vol. 13, pp. 110882-110899, 2025. [[CrossRef](#)] [[Google Scholar](#)] [[Publisher Link](#)]
- [15] Junyi Huang, M. Shirazi, and Xun Gong, "A New Arraying Technique for Band-Switchable and Polarization-Reconfigurable Antenna Arrays with Wide Bandwidth," *IEEE Open Journal of Antennas and Propagation*, vol. 3, pp. 1025-1040, 2022. [[CrossRef](#)] [[Google Scholar](#)] [[Publisher Link](#)]
- [16] Wanchen Yang et al., "Advanced Metasurface-Based Antennas: A Review," *IEEE Open Journal of Antennas and Propagation*, vol. 6, no. 1, pp. 6-24, 2025. [[CrossRef](#)] [[Google Scholar](#)] [[Publisher Link](#)]
- [17] Htet Wai Htun, Eisuke Nishiyama, and Ichihiko Toyoda, "A Single-Layer Planar Array Antenna Using Circularly-Polarized Reconfigurable Elements for Conical-Beam Radiation," *IEEE Access*, vol. 12, pp. 125306-125318, 2024. [[CrossRef](#)] [[Google Scholar](#)] [[Publisher Link](#)]
- [18] Sangeetha Subbaraj, and Shweta B. Thomas, "Reconfigurable Antennas and Their Practical Applications - A Review," *Radio Science*, vol. 58, no. 9, pp. 1-13, 2023. [[CrossRef](#)] [[Google Scholar](#)] [[Publisher Link](#)]
- [19] D. Ram Sandeep et al., "Functional Analysis in the Body Environment for a Circularly Polarized Hybrid Reconfigurable Textile Antenna," *Physica Scripta*, vol. 98, no. 10, 2023. [[CrossRef](#)] [[Google Scholar](#)] [[Publisher Link](#)]
- [20] Changying Wu et al., "Methodology to Reduce the Number of Switches in Frequency Reconfigurable Antennas with Massive Switches," *IEEE Access*, vol. 6, pp. 12187-12196, 2018. [[CrossRef](#)] [[Google Scholar](#)] [[Publisher Link](#)]